Heliyon 9 (2023) e16614

Contents lists available at ScienceDirect

Heliyon

journal homepage: www.cell.com/heliyon

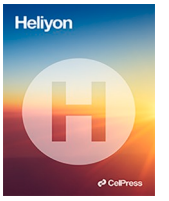

Research article

Improved defluoridation and energy production using dimethyl sulfoxide modified carbon cloth as bioanode in microbial desalination cell

Sabarija A. Mohandas [a], Sravan Janardhanan [a], P Abdul Rasheed [b,c], Praveena Gangadharan [a,d,*]

[a] Department of Civil Engineering, Indian Institute of Technology, Palakkad, Kerala, 678557, India
[b] Department of Biological Sciences and Engineering, Indian Institute of Technology, Palakkad, Kerala, 678557, India
[c] Department of Chemistry, Indian Institute of Technology, Palakkad, Kerala, 678557, India
[d] Environmental Sciences and Sustainable Engineering Centre, Indian Institute of Technology, Palakkad, Kerala, 678557, India

ARTICLE INFO

Keywords:
Defluoridation
Microbial desalination cell
Dimethyl sulfoxide
Oxygen functionalization
Wastewater treatment
Bioelectricity production

ABSTRACT

In the present study, carbon cloth (CC) was functionalized using dimethyl sulfoxide (DMSO) and employed as an excellent bioanode for improving defluoridation efficiency, wastewater treatment, and power output from a microbial desalination cell (MDC). The Raman spectroscopy and X-ray photoelectron spectroscopy (XPS) analysis of DMSO modified carbon cloth (CC_{DMSO}) confirmed the functionalization of CC_{DMSO}, and the water drop contact angle of 0° ensured its superior hydrophilicity. The presence of –COOH (carboxyl), S═O (sulfoxide) and *O*–C═O (carbonyl) functional groups on CC_{DMSO} aids in enhancing the performance of the MDC. Besides, cyclic voltametric and electrochemical impedance analysis revealed that CC_{DMSO} had an excellent electrochemical performance with low charge transfer resistance. Replacing CC with CC_{DMSO} as anode in MDC, the time required for 3,10 and 20 mg/L of initial fluoride (F^-) concentrations in the middle chamber was reduced from 24 ± 0.75 to 17 ± 0.37, 72 ± 1 to 48 ± 0.70, and 120 ± 0.5 to 96 ± 0.53 h, respectively to meet the prescribed standards (1.5 mg/L). Furthermore, using CC_{DMSO}, the anode chamber of MDC exhibited a maximum of 83% substrate degradation, and simultaneously, the power output is increased by 2–2.8 times. CC_{DMSO} improved the power production from 0.009 ± 0.003, 1.394 ± 0.06 and 1.423 ± 0.15 mW/m^2 to 0.020 ± 0.07, 2.748 ± 0.22 and 3.245 ± 0.16 mW/m^2, respectively, for initial F^- concentrations of 3,10, and 20 mg/L. Modifying CC with DMSO thus proved to be an efficient and simple methodology for enhancing the overall performance of MDC.

Abbreviations: MDC-Microbial desalination cell, CC-Carbon cloth; AEM-Anion exchange membrane, DMSO-Dimethyl sulfoxide; CEM-Cation exchange membrane, EIS-Electrochemical impedance spectroscopy; CV-Cyclic voltammetry, COD-Chemical oxygen demand; XPS-X-ray photoelectron spectroscopy, XRD-X-ray diffractometer; ISE-Ion selective electrode, FESEM-Field emission scanning electron microscopy; HR-, High resolution.

* Corresponding author. Department of Civil Engineering, Indian Institute of Technology, Palakkad, Kerala, 678557, India.
E-mail address: praveenag@iitpkd.ac.in (P. Gangadharan).

https://doi.org/10.1016/j.heliyon.2023.e16614
Received 25 October 2022; Received in revised form 9 May 2023; Accepted 22 May 2023
Available online 27 May 2023

Table 1
Comparison of carbon cloth (CC) anode modification procedures adopted in different bioelectrochemical systems.

Sl. No	Material used for CC modification	Modification method	Ref
1	Iodine (I_2) doped polythiophene nanoparticles (PTh –NP)	1. Doping of I_2 onto PTh 2. Dip dry method coating of doped PTh and I_2 onto CC	[38]
2	N-doped C/Fe_3O_4 nanotube	1. Hydrothermal deposition of nanowire template onto CC 2. Synthesis of precursor 3. Dipping in $FeCl_3$ to form FeOOH nanotube arrays on CC 4. Dipping in glucose and heating of CC-FeOOH to form C/Fe_3O_4-nanotube on CC	[39]
3	Iron nanostructure was synthesized on CC by electroplating	Electroplating in 0.16 M $FeCl_3$ solution at 5 V for 2 min using CC as cathode.	[40]
4	MnO_2, Pd and Fe_3O_4 nanoparticles	1. Synthesis of nanoparticles 2. Loading onto CC using binder	[41]
5	Atmospheric-pressure plasma jet processed reduced graphene oxides	1. Preparation of reduced graphene oxide paste (rGO) 2. Screen printing of rGO onto CC 3. Annealing using Atmospheric-pressure plasma jet	[42]
6	Atmospheric-pressure plasma jets.	Using N_2 at an operational voltage of 275 V	[43]

1. Introduction

Geogenic-originated groundwater pollution is a topic of major concern, and fluoride (F^-) stands first among them. F^- is introduced into the environment by both natural (rocks containing F^-, volcanic ash) and anthropogenic sources (industrial effluents from glass, phosphate fertilizers, semiconductors etc.) [1]. Unlimited tapping of groundwater also accelerates the leaching of F^- into the groundwater [2]. Drinking water with F^- concentrations up to 1.5 mg/L is advantageous as it checks dental decay, but concentrations >1.5 mg/L leads to chronic diseases like dental fluorosis and skeletal fluorosis [3]. The Geographical Survey of India has branded several areas under the "fluoride red alert" category, for instance, a concentration as high as 21 ppm was reported in Andhra Pradesh, India [4]. In recent years, more incidences of dental caries, twisted limbs, and yellow teeth have been reported among people of all ages in India [5]. As fluorosis is a prevalent disease, defluoridation of drinking water is highly essential for arresting the endemic effects on human health and physiology.

Several efficient methodologies are in existence for the defluoridation of groundwater. Defluoridation can be accomplished by coagulation and precipitation [6], membrane separation processes [7], adsorption [8–10], electro-dialysis [11], and electro coagulation [12,13]. Although the traditional treatment techniques improve water quality, most of them are either energy-intensive or demands chemical addition, which eventually generate large amounts of sludge [14]. The produced sludge requires further treatment prior to disposal. For instance, in conventional Nalgonda technique 1 kg of alum and 0.5 g of lime produces approximately 0.37 kg and 0.4 kg of sludge respectively [6]. Hence, it necessitates switching to a viable energy-positive technology with a reduced burden of secondary pollutants.

Recently, microbial desalination cells (MDCs) have gained wide attention as they are capable of desalinating water while simultaneously treating wastewater with energy recovery [15,16]. The MDC is a three chambered reactor consisting of an anodic chamber followed by a desalination chamber. An anion exchange membrane (AEM) is used to separate the two chambers. A cathodic chamber is provided after the desalination chamber, and the chambers are parted by a cation exchange membrane (CEM). MDC works on the principle of oxidation of organic matter by microbes in the anolyte and reduction of oxygen in the catholyte, resulting in a maximum electric potential gradient of 1.1 V (acetate = 16.9 mM; pH = 7; oxygen = 0.2 atm. (partial pressure)) [17,18]. The generated electric field drifts the anions (Na^+) and cations (Cl^-) through AEM and CEM, respectively, to anolyte and catholyte, resulting in water desalination in the middle chamber [19]. Using MDC, desalination can be achieved without applying pressure, or use of draw solutions, and/or the consumption of electrical energy. MDCs are flexible in treating various pollutants as they are unaffected by the nature of ions to be removed from contaminated water. Hence, research has been directed to use of MDCs for water softening [20,21], heavy metals removal [22–25], etc. However, its application in defluoridation has not been explored very much [23,24].

Although MDC is a promising technique for contaminant removal, its overall performance is severely affected by the properties of the anode, which are crucial for the development of exoelectrogenic microbes [26]. The major characteristics for the anode are biocompatibility, high porosity, specific surface area, conductivity, mechanical and chemical stability, and low cost [27]. In MDC, commonly used anodes are carbonaceous materials like carbon felt, carbon cloth, carbon brush, graphite rods, etc. [28]. Popular among them is carbon cloth (CC), as it is biocompatible and has good conductivity for efficient electron transfer [29,30]. Application of CC electrodes is hindered due to overpotential losses associated with limited active sites and poor hydrophilicity [31,32]. Recent studies have shown that these shortcomings might be resolved by appropriately activating the electrode surface of CC; as a result, more electrons can be transmitted with high power output. Numerous activation techniques, such as surface functionalization through the introduction of different functional groups, heteroatom doping, porous structure and morphology engineering, etc., have been reported in order to improve the physical and electrochemical properties of CC [33,34]. Among these, surface functionalization of CC is a viable option as the process is simple and it reduces the activation energy at the electrode-electrolyte interface [35,36]. Although the functionalization improves the overall performance of the electrode, the major challenge/constrains lies in the modification procedure. Most of the modification processes are either complicated, energy intensive, or require catalysts for efficient functioning [37],

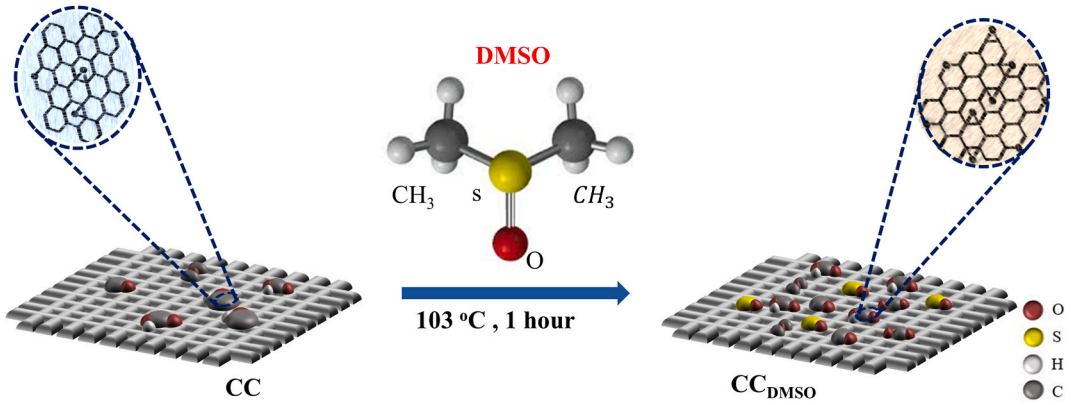

Fig. 1. Schematic representation of the principle of coating dimethyl sulfoxide (DMSO) onto carbon cloth (CC).

as given in Table 1.

Introducing active functional groups like amine (-NH_2), hydroxyl (-OH), carboxyl (-COOH), carbonyl (-C═O), etc., on to the surface of carbon electrodes has been performed by common methods like acid and thermal treatment, CO_2 activation, electrochemical methods, etc. [44,45]. Recently, incorporation of oxygen-containing functional groups on carbon-based electrodes has gained popularity due to its extraordinary ability to improve the catalytic activity, surface area and electrochemical properties of CC [46,47]. Dangling bonds and structural flaws are added to the carbon structure by oxygen functional groups. This leads to an increase in surface area and a decrease in activation energy between the electrode and electrolyte. Due to the binding of polar groups such as *C*–OH and –COOH, a strongly hydroxylated surface will be formed. This enhances the affinity for water [46]. The enhanced hydrophilicity of electrodes in polar solvents, as a result, improves the biocatalytic activity by increasing the electron transfer between microbes and anodes [48]. Oxygen functional groups can be incorporated by treating CC with compounds like nitric acid [46], potassium ferrate [45], benzoyl peroxide [47], etc. However, these processes require multiple levels of treatment that include strong acids and/or noble metals. Hence, selecting an appropriate compound that can modify CC in a facile way is imperative.

In this work, an attempt has been made to effectively functionalize the surface of CC in a simple step using dimethyl sulfoxide (DMSO). DMSO is one such compound that enables facile introduction of an O containing functional group onto the CC surface [49]. DMSO – a common laboratory and industrial reagent, is an outstanding solvent for both organic and inorganic materials and has excellent electrochemical properties [50]. Unlike the existing complex CC modification methods as given in Table 1, DMSO can be easily applied to CC in a single step without affecting the structure of CC. To the best of our knowledge the possibility of facile modification of CC using a common laboratory/industrial solvent for bioelectrochemical applications has not been reported. The objective of the present study is to explore the feasibility of using DMSO modified CC (CC_{DMSO}) as an anode in MDC and compare its performance with unmodified CC for defluoridation, wastewater treatment, and power output.

2. Materials and methods

2.1. Materials

CC was procured from Sainergy fuel cell India Pvt. Ltd. and ion exchange membranes (AEM, CEM) from Ralex ion exchange membranes, India. Analytical grade chemicals - NH_4Cl, NaCl, $CaCl_2$, $MgSO_4$, $NaHCO_3$, KH_2PO_4, K_2HPO_4, NaF, $CaCl_2.2H_2O$, $MgCl_2.6H_2O$, NaF, and sodium acetate were obtained from Sigma Aldrich, India, and DMSO from Merck, India. All the materials were used without any purification or treatment.

2.2. Coating dimethyl sulfoxide onto electrodes

Commercially available DMSO was coated onto CC using the drop cast method [51]. CC of size 3.5 × 3.5 cm^2 were rinsed in deionized water and heated at 100 °C until completely dry. 5 mL of DMSO was applied to the oven dried CC, drop by drop, until the electrode was fully immersed in the solvent. This was allowed to remain in contact for 30 min at room temperature, followed by oven drying at 100 °C for 1 h. The schematic representation of the principle of coating DMSO onto CC is shown in Fig. 1. The modified electrodes were stored in a desiccator before use.

2.3. Reactor setup

A three chambered MDC reactor was fabricated using acrylic sheets. The reactor constitutes of three identical chambers, each of 100 mL capacity. The first one being the anode chamber, followed by a chamber for defluoridation in the middle, and finally the cathode chamber. The chambers were separated by an AEM (3.14 cm^2) between the middle and the anode chambers, and a CEM (3.14

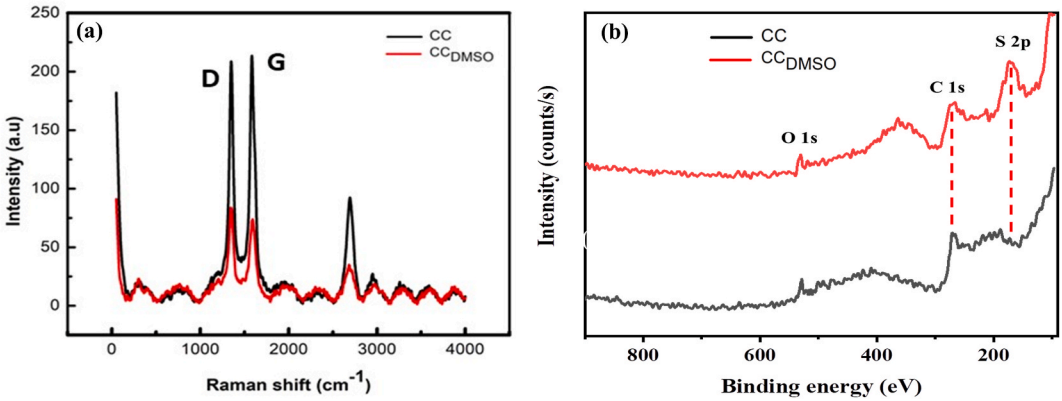

Fig. 2. (a) Raman spectrum and (b) X-ray photoelectron spectroscopic survey spectra of carbon cloth (CC) and dimethyl sulfoxide modified carbon cloth (CC_{DMSO}).

cm^2) between the cathode and the middle chambers. The reactor was made water and airtight using O-rings and clamped with stainless steel bolts. Sampling ports were provided on the top of each chamber. CC_{DMSO} and CC (control) were used as anodes (3.2 × 3.2 cm^2), and CC was used as the cathode (3.2 × 3.2 cm^2) in both cases. The electrodes were coupled physically with copper wire across a 1 Ω resistor (high current mode).

2.4. Inoculation and operation

The anode chamber was filled with synthetic wastewater. The anolyte (per L of Milli-Q water, 18.2 MΩ) was prepared using: NH_4Cl, 0.11 g; KCl, 0.036 g; $MgSO_4{\cdot}7H_2O$, 0.09 g; $CaCl_2{\cdot}2H_2O$, 0.014 g; yeast extract, 0.001 g; and 0.3 mL of trace elements [52]. The reactor was inoculated with anaerobically digested sludge, which was obtained from an effluent treatment plant in Ahalya Medical College, Palakkad, India. Sodium acetate was used as the carbon source for the microbes. Nitrogen gas was purged continuously to maintain anaerobic conditions in the anode chamber. Aerated phosphate buffer prepared using KH_2PO_4 (0.53 g/L); and K_2HPO_4 (1.07 g/L) (per L of Milli-Q water) was used as the catholyte [21]. 3, 10, and 20 mg/L of F^- solutions were synthetically readied by dissolving reagent grade NaF in deionized water and were added to the middle desalination chamber [7].

2.5. Measurements and analyses

pH and F^- were measured in a pH/ion selective electrode (ISE) (Thermo Scientific Orion Star A214 pH/ISE). Conductivity was monitored using a benchtop conductivity meter (Thermo Scientific Orion Star A222, portable conductivity meter). The COD (substrate degradation efficiency) of anolyte was measured using the closed reflux method as described in the standard method (APHA, 2012). The substrate degradation and defluoridation efficiencies were determined using Eq. (1).

$$\text{Removal efficiency } (\%) = \frac{A - B}{A} \times 100 \tag{1}$$

where, A and B are the initial and final concentration of contaminant, respectively.

Voltage (V) was monitored using a data logger (DAQ6510, Keithley). As per Ohm's law, current (I)=V/fixed resistance. Corresponding to a particular external resistance, the current density (mA/m^2) was estimated by dividing I and power density (mW/m^2) by dividing VI by the effective area of anode (m^2). Polarization study was conducted by manually varying the external resistance from 1 Ω to 10.2 MΩ.

2.6. Characterization of the modified electrodes

The macroscale distribution of DMSO on CC was examined using a Raman spectrophotometer (Horiba Labram HR Evo), and the surface chemistry was investigated by X-ray photoelectron spectroscopy (XPS) (ULVAC-PHI Inc. Model: PHI5000 Version Probe III). The water drop contact angle measurements were done by an optical angle measurement device (Holmarc contact angle meter, HO-IAD-CAM-01A). The surface image of the modified CC was obtained using field emission scanning electron microscopy (FESEM) (Carl Zeiss, Gemini SEM 300), and X-ray diffraction peaks were noted in the scanning window of 10°–60° by a diffractometer (XRD Smart Lab, Rigaku).

The electrochemical analysis of electrodes was performed as a three-electrode system using a Potentiostat (Multi Autolab M204, Metrohm) and NOVA 2.1 software. The working electrode used was CC/CC_{DMSO}, while platinum wire being the counter electrode, and the reference electrode chosen was a saturated calomel electrode in an electrolyte solution prepared using potassium ferricyanide (5 mM), phosphate buffer (5 mM), and KCl (0.1 M). Cyclic voltametric (CV) analysis was carried out from 0.1 V to 1 V, and the scan rate

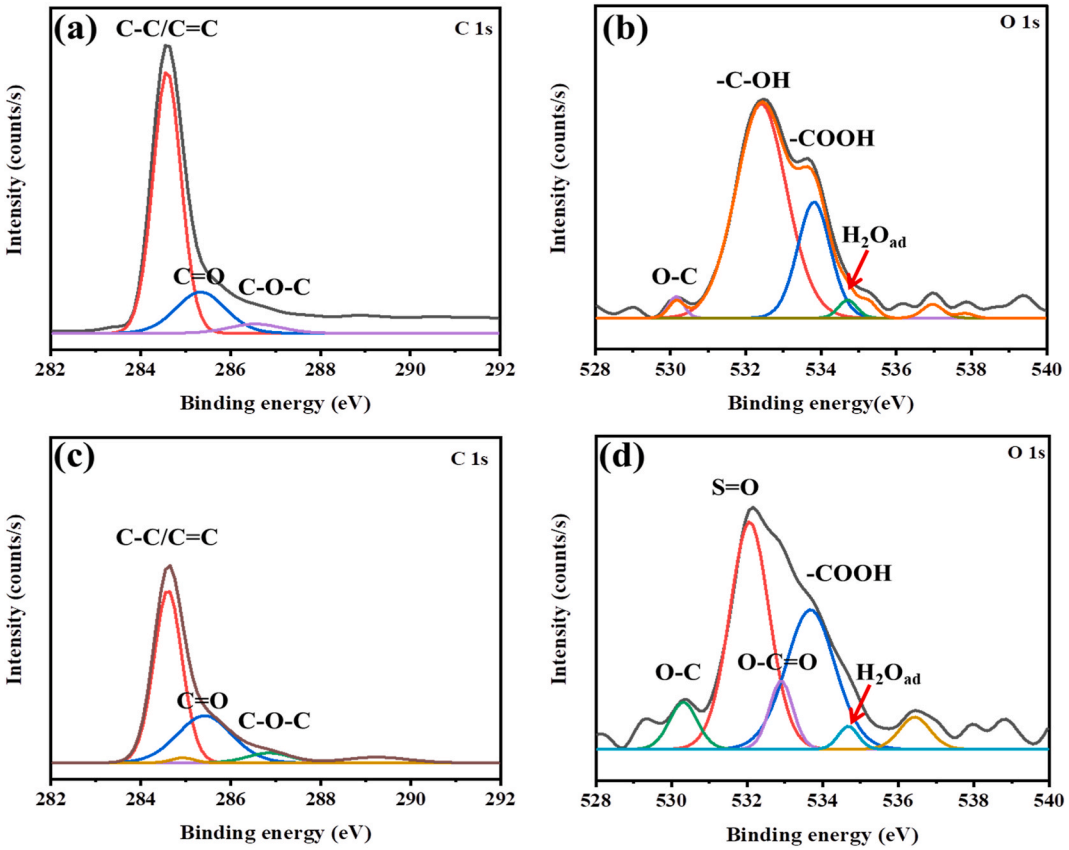

Fig. 3. The HR scans for (a) C 1s and (b) O 1s for CC, (c) C 1s and (d) O 1s for dimethyl sulfoxide modified carbon cloth (CC_{DMSO}).

was fixed at 0.02 V/s. Electrochemical impedance spectroscopic (EIS) analyses were done in the frequency range of 0.1 Hz–10^5 Hz with an amplitude of 0.1 V. The equivalent circuit of the EIS spectra was simulated to determine charge transfer resistance (R_{ct}) in the software ZSimpwin 3.21.

3. Results and discussion

3.1. Chemical characterization of carbon cloth and dimethyl sulfoxide modified carbon cloth

Raman spectra of CC_{DMSO} show an increase in the I_D/I_G of CC_{DMSO} (1.106) compared to CC (0.94), indicating a lower level of graphitization and a more disorganized structure. This process, is crucial in the introduction of functional groups like –COOH and –OH onto the electrode surface and causes more flaws and dangling bonds (Fig. 2a) [46]. The obtained results follow the same pattern as those obtained in the study by Ref. [53] which reported an increase in the I_D/I_G value when graphene was doped with nitrogen. The effectiveness of reduction and chemical composition (C 1s and O 1s) of CC and CC_{DMSO} were evaluated by XPS (Fig. 2b). The CC_{DMSO} showed an additional peak for S 2p, which can be derived from the S atom present in DMSO.

The high resolution (HR) scan of C 1s of CC shows a sharp and minor peak at 284.6 eV and 284.9 eV, respectively, caused by the *C*–C/C═C group [39,48]. A peak at 285.4 eV observed on CC can be attributed to the C═O group, and a small peak at 286.9 eV could be related to the *C*–*O*–C group [49,50]. CC_{DMSO} also exhibited similar peaks, however, after modification, the C═O and *C*–*O*–C peaks were found to be enhanced, while the intensity of the peak for *C*–C/C═C was reduced. The HR scan of O 1s of CC (Fig. 3a) shows peaks at 532.5 eV and 533.7 eV that can be attributed to the –C-OH and –COOH groups, respectively [46]. Additionally, a small peak that corresponds to the presence of *O*–C is observed at 530.3 eV [54] (Fig. 3b). The HR scan of C 1s of CC_{DMSO} shows a similar peak of *O*–C at 530.3 with higher intensity, which confirms the attachment of oxygen during modification (Fig. 3c). Similarly, the intensity of –COOH peak is enhanced after the DMSO modification. An additional peak at 532.9 eV is observed after DMSO modification, which can be attributed to *O*–C═O [54] (Fig. 3d). The enhancement in the peaks of *O*–C and –COOH along with the new peak for *O*–C═O and S═O confirms the functionalization after the treatment. The peak observed at 532 eV in the CC_{DMSO} originates from the S═O of DMSO [55]. A peak at 534.6 eV is observed in both samples, which corresponds to adsorbed H_2O on the CC surface [56].

The surface hydrophilicity of CC and CC_{DMSO} was investigated by performing the waterdrop contact angle measurement (Fig. 4). The contact angle between deionized water and CC was 132.2° (Fig. 4a). DMSO lowered the contact angle to 123.4° within 15 min

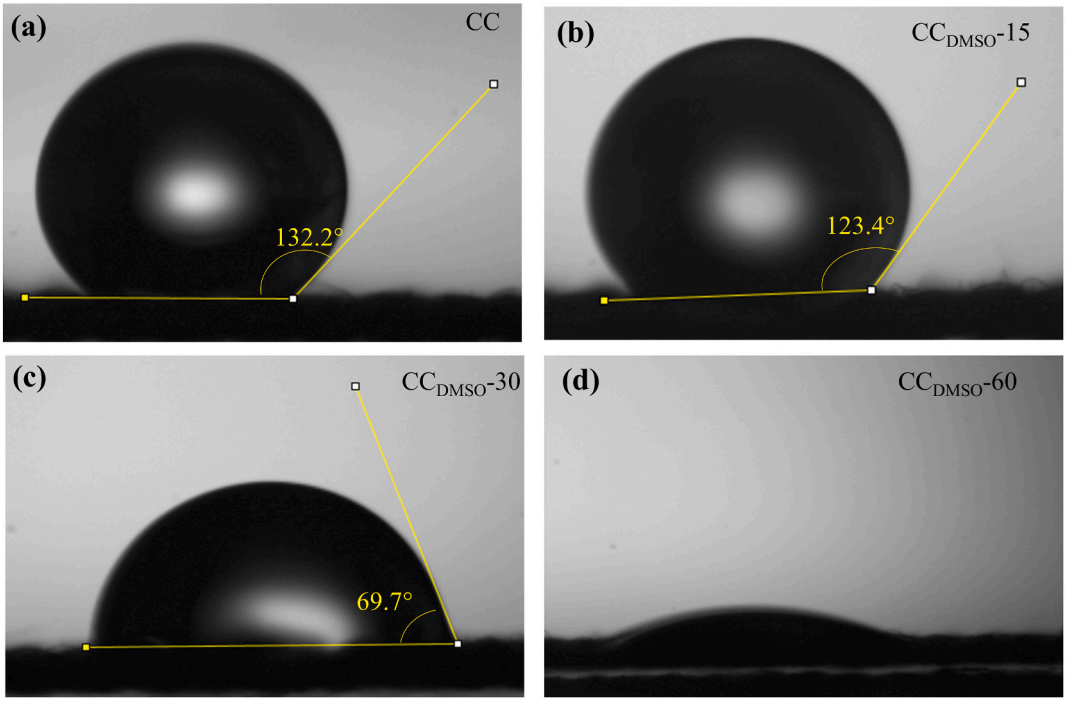

Fig. 4. (a) The waterdrop contact angle of bare carbon cloth (CC). The waterdrop contact angle of dimethyl sulfoxide modified carbon cloth after: (b) 15 min contact time (CC_{DMSO} – 15); (c) 30 min contact time (CC_{DMSO} – 30); and (d) 60 min contact time (CC_{DMSO} – 60).

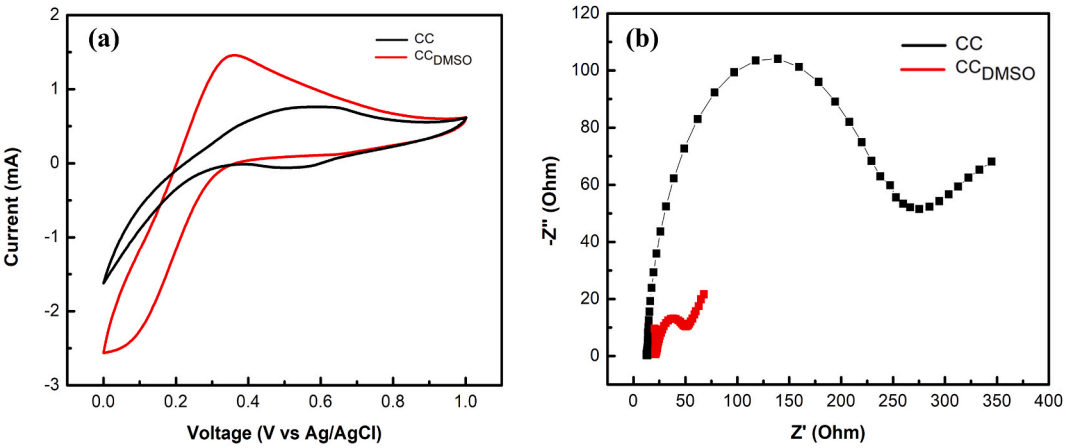

Fig. 5. (a) Cyclic Voltametric and (b) Nyquist curves.

(Fig. 4b) of contact time. The angle further reduced to 69.7° after 30 min (Fig. 4c) of contact with DMSO. The contact angle was 0° when the time of dip of CC in DMSO was increased to 60 min (Fig. 4d), attributed to the superior wetting phenomenon of CC_{DMSO}. The hydrophilic property of CC_{DMSO} was contributed by the presence of –COOH and -*C*-OH functional groups [42].

The SEM analysis for structural characterization revealed that the application of DMSO did not cause any changes to the morphology of CC (Fig. S1a and S1b). Little change in the characteristic peak intensity and position in the XRD patterns of CC and CC_{DMSO} (Fig. S_2) highlights that DMSO did not alter the structural characteristics of CC. The two characteristic peaks at 25.8° and 43.7° can be assigned to the (002) and (101) diffraction peaks of graphitic carbon of CC [57].

3.2. Electrochemical characterization of carbon cloth and dimethyl sulfoxide modified carbon cloth

In the electrochemical analysis, CC_{DMSO} exhibited a higher anodic current density (~1.45 mA) than CC (~0.75 mA). The improved response of CC_{DMSO} can be correlated with the reduced overpotential loss owing to the enhanced electron transfer and superior

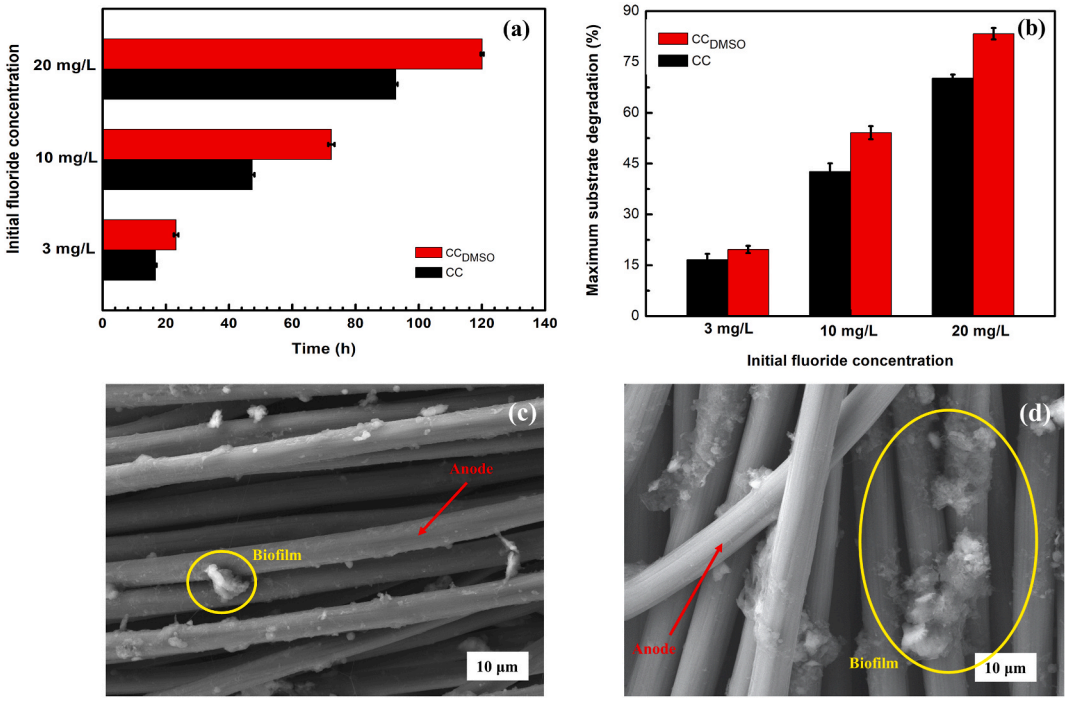

Fig. 6. (a) Time taken to achieve permissible limit of 1.5 mg/L of fluoride. (b) Maximum substrate degradation obtained. (c) SEM image of biofilm on carbon cloth (CC) anode, and (d) SEM image of denser biofilm on dimethyl sulfoxide modified carbon cloth (CC_{DMSO}) anode.

hydrophilic property [35]. The CC did not exhibit distinct redox peaks (Fig. 5a), signifying the presence of electric double-layer capacitive characteristics and the non-availability of considerable redox mediators, whereas a single peak was evident in the case of CC_{DMSO} [58]. The higher area under the CV curve and peak current of CC_{DMSO} could be owing to an increase in the available electroactive sites that enhance the charge transfer capability [59,60]. This implies that coating DMSO onto CC increases the number of available attachment sites for microbes and the electrochemically active surface area, which is an important requisite for a high-performance anode in MDC [39].

The Nyquist curves of electrodes before and after modification with DMSO are given in Fig. 5b. It comprises three sections indicating: (i) ohmic resistance - an intercept at high frequency; (ii) charge transfer resistance (R_{ct}), – diameter of the semicircle part; and (iii) Warburg diffusion, - straight line portion at low frequencies. The R_{ct} value of CC_{DMSO} is noticeably lower (23 Ω) than that of CC (175 Ω), indicating a decline in the resistance for charge transfer at the electrode–electrolyte interface of CC_{DMSO} [61]. The charge transfer resistance of CC_{DMSO} was reduced due to the combined effects of good electrical conductivity, wettability, and the superior electrocatalytic properties of DMSO. All the mentioned factors help in improving the electrolyte - electrode interfacial characteristics and thus lowering the internal resistance and mass transfer losses [35]. Improving the charge transfer rate can result in reducing the energy of activation required for initiating the redox reactions [31].

3.2. *Defluoridation and wastewater treatment*

The CC and CC_{DMSO} were employed as anodes in MDCs, and their performance in defluoridation and wastewater treatment were investigated. The defluoridation efficiency was evaluated by monitoring the time required to reduce the F^- concentration to the prescribed standard limit of 1.5 mg/L. A significant enhancement in the performance of MDC for defluoridation was observed when the CC anode was replaced with CC_{DMSO}. Using CC as a bioanode, 3, 10, and 20 mg/L of F^- ions in the middle chamber took 24 ± 0.75, 72 ± 1, and 120 ± 0.5 h, respectively, to reach the permissible level (1.5 mg/L). However, with CC_{DMSO}, the same level of treatment was achieved within 17 ± 0.37, 48 ± 0.70, and 96 ± 0.53 h for 3,10 and 20 mg/L, respectively (Fig. 6a).

Ionic separation at the middle chamber of MDC occurs due to the electric potential gradient generated by the anode and cathode. The presence of functional groups such as –COOH, *O*–C, *O*–C═O, and S═O groups on CC_{DMSO} indicates extensive functionalization of the CC surface. Eventually, the wettability and electrochemical activity of the electrode were improved, resulting in a high electric potential gradient across the electrode. Due to hydrogen bonding between the –COOH functional group and the membrane-bound peptide bonds in the bacterial cytochromes (that are linked to the intracellular electron transfer chain), the exoelectrogenic activity of the microbes was improved [42]. This eventually increases the potential gradient. As the potential gradient and ionic removal are correlated, the migration of F^- ions in the middle chamber was accelerated to the anode chamber with a CC_{DMSO} anode [46]. In addition to the potential gradient, the concentration gradient also plays a major role in the defluoridation. Initially, the concentration gradient would be sufficiently high to accelerate the rate of ion diffusion [62]. The concentration gradient decreases with time due to

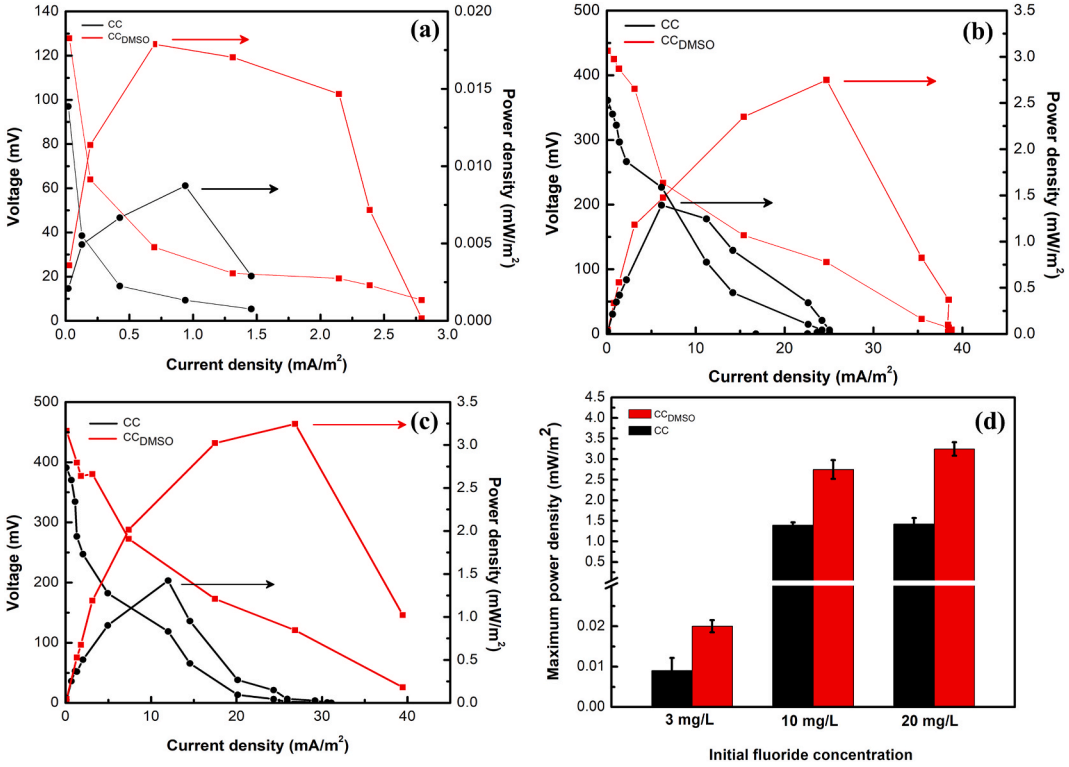

Fig. 7. Polarization profiles of (a) 3 mg/L, (b) 10 mg/L, (c) 20 mg/L fluoride using carbon cloth (CC) and dimethyl sulfoxide modified carbon cloth (CC_{DMSO}) anode and (d) maximum power density comparison.

the movement of ions into the anolyte. This automatically reduces the rate of ion diffusion, and as a result, higher F^- concentrations take more time to reach 1.5 mg/L. Therefore, the rate of defluoridation in MDC can primarily be attributed to the potential and the concentration gradient between the middle and the adjacent chambers.

Simultaneously, the substrate degradation in the anode chamber of MDC was examined for CC and CC_{DMSO}. The maximum COD removal was found to increase from 16.7 ± 1.7 to 19.66 ± 3.5% with 3 mg/L of initial F^-, from 42.6 ± 2.47 to 54.1 ± 1.92% with 10 mg/L of initial F^-, and from to 70.2 ± 1.09 to 83 ± 1.68% with 20 mg/L of initial F^- using CC and $CC_{DMSO,}$ respectively (Fig. 6b). The improved hydrophilicity and electrochemically active sites of CC_{DMSO} facilitate more bacterial colonization, and as a result, enhanced substrate degradation can be obtained [43]. This was further validated with the SEM analysis of electrodes used in MDC. The results revealed that the thickness and abundance of biofilm were found to be greater on CC_{DMSO} (Fig. 6d) than on CC (Fig. 6c).

The high defluoridation and COD removal efficiency of CC_{DMSO} could be due to (i) the presence of –COOH, *O*–C, -*C*-OH and *O*–C═O functional groups on CC_{DMSO}, which reduced the overpotential losses associated with the oxidation of organic substrates [44]; (ii) the higher hydrophilicity of CC_{DMSO} improves the biocompatibility of anodes, which allows rapid attachment of microorganisms to the anode surface; and (iii) the enhanced wettability of DMSO, which increases the interaction between microbes, substrates, and electrode, as a result, the organic matter is degraded more effectively.

3.3. Power production

The performance of CC and CC_{DMSO} in MDC for power production was examined at initial F^- concentrations of 3, 10, and 20 mg/L. The optimal power density for CC and CC_{DMSO} was obtained by conducting polarization studies. The maximum power densities achieved for CC_{DMSO} at 3, 10, and 20 mg/L was 0.020 ± 0.07, 2.748 ± 0.22 and 3.245 ± 0.16 mW/m^2, respectively. However, using CC, lower power densities of 0.009 ± 0.003, 1.394 ± 0.06 and 1.423 ± 0.15 mW/m^2, were obtained respectively, with 3 (Fig. 7a), 10 (Figs. 7b), and 20 mg/L (Fig. 7c) of F^-. The obtained results are in good agreement with the defluoridation efficiency and substrate degradation as described in the previous sections.

The presence of hydrophilic functional groups on the CC_{DMSO} anode reduced overpotential losses associated with the oxidation of organic substrates and improved electrode-microbe interaction, leading to higher power production than CC. The higher power output can also be correlated to the low R_{ct} and the higher redox peak intensity of CC_{DMSO}. Both the parameters resulted in a drastic improvement in the electron transfer from the microorganisms to the anode surface [39,40] which benefited the energy output from MDC.

In MDC, the power production is severely affected by: (i) the bioelectrochemical process driven by microbes in the anode chamber;

Table 2
Comparison of different defluoridation techniques.

Sl. No	Technique	Energy	Chemical requirement	Performance	Reference
1	Enhanced Nalgonda technique	(−)* 230 V/240 V, 20 min	1 g/L alum + 0.15 g/L lime + 0.05 g/L Aluminium hydroxide + NaOH for pH adjustment	9.3 mg/L F^- reduced to 2.8 mg/L in 5 h	[6]
2	Electrolytic defluoridation (EDF)	(−)* 16 V, 4 h	____	7.9 mg/L F^- reduced to 2.8 mg/L in 4 h	[6]
3	Adsorption	(−)*	1 g pulverized spent cation exchange resin + Zn (IV) powder	12.2 mg/L F^- reduced to 1.5 mg/L in 24 h	[8]
4	Electrodialysis	(−)* 12 V, 21 h 30 min	____	3.94 mg/L F^- reduced to 0.283 mg/L in 21 h 30 min	[11]
5	Electrocoagulation	(−)* 4 mA/m^2, 15 min	____	2.5 mg/L F^- reduced to 1.5 mg/L in 3 h	[13]
6	Microbial desalination cell (MDC)	(+)* 3.245 ± 0.16 mW/m^2	____	3 mg/L F^- —17, 10 mg/L F^- —48, 20 mg/L F^-– 96 h to reach 1.5 mg/L	Present study

* Energy consumed (−), Energy produced (+).

and (ii) the concentration of ions in the middle chamber of MDC [20,35]. With the increase in F^- from 3 to 20 mg/L, the power output also improved from 0.009 ± 0.003 to 1.423 ± 0.15 mW/m^2 and from 0.020 ± 0.07 to 3.245 ± 0.16 mW/m^2 for CC and CC_{DMSO}, respectively. Similar results have been reported by Jafary et al. [63]. The ionic diffusion driven by the concentration gradient between the chambers could be a possible reason for this phenomenon [15,20]. With the increase in the concentration of ions in the middle chamber, the concentration gradient across the anode and middle chamber also increases. This would cause the diffusion of more ions at higher concentrations of F^- than at lower concentrations. High current generation resulted from a faster desalination rate, while low current generation from a slow desalination rate. Generally, it has been reported that the electrical gradient is the primary force at low salt concentrations, whereas the concentration gradient is dominant at high salt concentrations in the middle desalination chamber [63]. This phenomenon results in increasing the conductivity in the anode chamber, which lowers the overall ohmic resistance of MDC [64]. Hence, the synergetic effect of biofilm, DMSO in CC, and reduced ohmic resistance of MDC improved the power output by 2–2.28 times (Fig. 7d). The results thus proved the effectiveness of the single step facile modification of CC by DMSO in functionalizing the CC electrode.

4. Conclusions and outlook

In the present study, a novel electrode was fabricated by coating a solvent - DMSO onto CC via a facile modification method. The CC_{DMSO} was used as an anode in the MDC for improved defluoridation, wastewater treatment, and power production. The presence of *O*–C, –COOH, *O*–C═O, *C*–OH, and S═O groups on CC_{DMSO} improved the conductivity and hydrophilicity of CC and resulted in an enriched microbial growth on the anode surface, as indicated in Fig. 6c and d. This might have improved the redox activity of the anode. Additionally, the higher redox peak and lower charge transfer resistance of CC_{DMSO} reduced the internal resistance of the anode and facilitated high power output from the MDC. Moreover, the MDC equipped with CC_{DMSO} bioanode considerably reduced the time taken to bring the F^- concentrations to the permissible limit (1.5 mg/L). Simultaneously, 83% of substrate degradation was obtained in the anodic chamber of MDC. CC_{DMSO} exhibited a higher power density, of approximately 2–2.28-fold higher than the CC electrode.

The utilisation of a lab scale MDC for defluoridating water was effectively proven in the current study. Compared with conventional techniques, MDC does not require the addition of chemicals or energy (Table 2). It is a self-sufficient system that uses a bio-electrochemical process to remove fluoride from water, treat wastewater, and recover energy, concurrently. Though MDC exhibits various applications, its long-term performance is hindered due to various factors. The major operating concern was the consistent drop in the ion migration rate over the time. This might be explained by the gradual increase in the internal resistance, caused by the ion transport across the membranes and membrane fouling [65]. Improving the membrane properties with antifoulant coatings or materials will help in boosting up the MDC performance. In addition, concentration polarization due to the back diffusion of ions from the electrolytes (anolyte and catholyte) to the middle chamber can further reduce its performance [66]. A continuous recirculation of electrolytes will reduce the adverse effects of concentration polarization.

Application of DMSO in MDC is a promising technique for defluoridation. Future research will be focused on the optimization of operational and design parameters to upscale MDC. A number of MDC configurations, such as stacked resin packed MDC [67], Up flow two chambered MDC [68], quadruple MDC [63], etc., have been investigated by various researchers, but the studies were limited to the desalination of brine or groundwater only. Future studies will be directed to analyse the sustainability and future impacts of upscaling MDC with electrode modification using DMSO and other nanoparticles (MXene [69], titanium dioxide nanosheets), conductive polymers (polypyrrole) [70] etc., for defluoridation. Tools like life cycle assessment (LCA), techno-economic analysis, emergy analysis (measures all the energy expended in producing a good or service in terms of a single type of energy), exergoeconomic analysis (involves both energy and the cost of the system) [71] will help in evaluating the overall sustainability and feasibility of the developed

systems. Furthermore, DMSO based electrodes can be explored in redox flow batteries, wearable sensors, etc., owing to their superior electrochemical properties.

Credit author statement

Sabarija A Mohandas: methodology, experimental analysis, data interpretation, validation, writing -original draft. **Sravan Janardhanan**: experimental analysis, data interpretation. **P Abdul Rasheed:** supervision, conceptualization, methodology, writing - review and editing - original draft. **Praveena Gangadharan:** supervision, funding acquisition, conceptualization, methodology, data interpretation, writing - original draft.

Data availability statement

Data will be made available on request.

Declaration of competing interest

The authors declare the following financial interests/personal relationships which may be considered as potential competing interests:

Praveena Gangadharan reports financial support was provided by Science and Engineering Research Board (SERB), India.

Acknowledgement

The authors gratefully acknowledge the financial support of the Science and Engineering Research Board (SERB) [No.EEQ/2018/000524 and ECR/2018/000601], Department of Science and Technology, Government of India in carrying out this research work. The authors would also like to thank Dr. Subramanyan Namboodiri Varanakkottu and Lekshmi B S, Optofluidics and Interface Science Laboratory, NIT Calicut, for contact angle measurements and the Central Instrumentation Facility, IIT Palakkad, for the remaining characterization studies.

Appendix A. Supplementary data

Supplementary data to this article can be found online at https://doi.org/10.1016/j.heliyon.2023.e16614.

References

[1] M.S. Gaikwad, C. Balomajumder, TFC polyamide NF membrane: characterization, application and evaluation of MTPs and MTC for simultaneous removal of hexavalent chromium and fluoride, E-Polymers 17 (2017) 129–136, https://doi.org/10.1515/epoly-2016-0219.
[2] N. Adimalla, S. Venkatayogi, S.V.G. Das, Assessment of fluoride contamination and distribution: a case study from a rural part of Andhra Pradesh, India, Appl. Water Sci. 9 (2019), https://doi.org/10.1007/s13201-019-0968-y.
[3] BIS, Indian standard drinking water specification (second revision), Bur. Indian Stand. IS 10500 (2012) 1–11. http://cgwb.gov.in/Documents/WQ-standards.pdf.
[4] N.C. Mondal, R.K. Prasad, V.K. Saxena, Y. Singh, V.S. Singh, Appraisal of highly fluoride zones in groundwater of Kurmapalli watershed, Nalgonda district, Andhra Pradesh (India), Environ. Earth Sci. 59 (2009) 63–73, https://doi.org/10.1007/s12665-009-0004-x.
[5] R. Rajumon, P. Gangadharan, S.A. Mohandas, Osmotic microbial fuel cell for groundwater softening, Defluoridation , Salinity Reduction , and Energy Production 149 (2023) 1–10, https://doi.org/10.1061/JOEEDU.EEENG-6995.
[6] L.Y. Teshome, F.C. Jim, Z.B. Feleke, A.S. David, Performance enhancement of Nalgonda technique and pilot testing electrolytic defluoridation system for removing fluoride from drinking water in East Africa, Afr. J. Environ. Sci. Technol. 12 (2018) 357–369, https://doi.org/10.5897/ajest2018.2545.
[7] A. Figoli, J. Hoinkis, J. Bundschuh, Membrane Technologies for Water Treatment: Removal of Toxic Trace Elements with Emphasis on Arsenic, Fluoride and Uranium, 2016, https://doi.org/10.1201/b19227.
[8] H. Paudyal, K. Inoue, H. Kawakita, K. Ohto, Removal of fluoride by effectively using spent cation exchange resin, J. Mater. Cycles Waste Manag. 20 (2018) 975–984, https://doi.org/10.1007/s10163-017-0659-4.
[9] V. Ganvir, K. Das, Removal of fluoride from drinking water using aluminum hydroxide coated rice husk ash, J. Hazard Mater. 185 (2011) 1287–1294, https://doi.org/10.1016/j.jhazmat.2010.10.044.
[10] N. Nabbou, M. Belhachemi, M. Boumelik, Comptes Rendus Chimie Removal of fl uoride from groundwater using natural clay (kaolinite): optimization of adsorption conditions, Compt. Rendus Chem. (2018) 1–8, https://doi.org/10.1016/j.crci.2018.09.010.
[11] S. Gmar, I. Ben, S. Sayadi, N. Helali, M. Tlili, M. Ben Amor, Desalination and Defluoridation of Tap Water by Electrodialysis, vol. 2, 2015, https://doi.org/10.1007/s40710-015-0112-4.
[12] M.M. Emamjomeh, M. Sivakumar, Fluoride removal by a continuous flow electrocoagulation reactor, J. Environ. Manag. 90 (2009) 1204–1212, https://doi.org/10.1016/j.jenvman.2008.06.001.
[13] I. Rodríguez, S. Guti, Chemosphere Arsenic and fl uoride removal from groundwater by electrocoagulation using a continuous fi lter-press reactor n a, Jos e 144 (2016) 1–8, https://doi.org/10.1016/j.chemosphere.2015.10.108.
[14] S. Manna, D. Roy, B. Adhikari, S. Thomas, P. Das, M.S. Centre, Biomass for water defluoridation and current understanding on biosorption mechanisms, A Review 00 (2018) 1–13, https://doi.org/10.1002/ep.12855.
[15] X. Cao, X. Huang, P. Liang, K. Xiao, Y. Zhou, X. Zhang, B.E. Logan, A new method for water desalination using microbial desalination cells, Environ. Sci. Technol. 43 (2009) 7148–7152, https://doi.org/10.1021/es901950j.
[16] H.M. Saeed, G.A. Husseini, S. Yousef, J. Saif, S. Al-Asheh, A. Abu Fara, S. Azzam, R. Khawaga, A. Aidan, Microbial desalination cell technology: a review and a case study, Desalination 359 (2015) 1–13, https://doi.org/10.1016/j.desal.2014.12.024.

[17] Y. Kim, B.E. Logan, Microbial desalination cells for energy production and desalination, Desalination 308 (2013) 122–130, https://doi.org/10.1016/j.desal.2012.07.022.
[18] M.J. Khan, V.J. Suryavanshi, K.B. Joshi, P. Gangadharan, V. Vinayak, in: M. El-Sheekh, A.E. FBT-H, A.B. Abomohra (Eds.), Chapter 16 - Photosynthetic Microalgal Microbial Fuel Cells and its Future Upscaling Aspects, Elsevier, 2022, pp. 363–384, https://doi.org/10.1016/B978-0-12-823764-9.00005-4.
[19] M. Mehanna, T. Saito, J. Yan, M. Hickner, X. Cao, X. Huang, B.E. Logan, Using microbial desalination cells to reduce water salinity prior to reverse osmosis, Energy Environ. Sci. 3 (2010) 1114–1120, https://doi.org/10.1039/c002307h.
[20] M. Hemalatha, S.K. Butti, G. Velvizhi, S. Venkata Mohan, Microbial mediated desalination for ground water softening with simultaneous power generation, Bioresour. Technol. 242 (2017) 28–35, https://doi.org/10.1016/j.biortech.2017.05.020.
[21] K.S. Brastad, Z. He, Water softening using microbial desalination cell technology, Desalination 309 (2013) 32–37, https://doi.org/10.1016/j.desal.2012.09.015.
[22] Z. An, H. Zhang, Q. Wen, Z. Chen, M. Du, Desalination combined with hexavalent chromium reduction in a microbial desalination cell, Desalination 354 (2014) 181–188, https://doi.org/10.1016/j.desal.2014.10.006.
[23] Z. An, H. Zhang, Q. Wen, Z. Chen, M. Du, Desalination combined with copper(II) removal in a novel microbial desalination cell, Desalination 346 (2014) 115–121, https://doi.org/10.1016/j.desal.2014.05.012.
[24] M. Malakootian, H. Mahdizadeh, A. Nasiri, F. Mirzaienia, M. Hajhoseini, N. Amirmahani, Investigation of the efficiency of microbial desalination cell in removal of arsenic from aqueous solutions, Desalination 438 (2018) 19–23, https://doi.org/10.1016/j.desal.2018.03.025.
[25] B. Zhang, C. Feng, J. Ni, J. Zhang, W. Huang, Simultaneous reduction of vanadium (V) and chromium (VI) with enhanced energy recovery based on microbial fuel cell technology, J. Power Sources 204 (2012) 34–39, https://doi.org/10.1016/j.jpowsour.2012.01.013.
[26] C. Feng, F. Li, H. Liu, X. Lang, S. Fan, A dual-chamber microbial fuel cell with conductive film-modified anode and cathode and its application for the neutral electro-Fenton process, Electrochim. Acta 55 (2010) 2048–2054, https://doi.org/10.1016/j.electacta.2009.11.033.
[27] T. Huggins, H. Wang, J. Kearns, P. Jenkins, Z. Jason, Bioresource Technology Biochar as a Sustainable Electrode Material for Electricity Production in Microbial Fuel Cells, vol. 157, 2014, pp. 114–119, https://doi.org/10.1016/j.biortech.2014.01.058.
[28] D. Nosek, P. Jachimowicz, A. Cydzik-Kwiatkowska, Anode modification as an alternative approach to improve electricity generation in microbial fuel cells, Energies 13 (2020) 1–22, https://doi.org/10.3390/en13246596.
[29] C. Wang, T. Sangeetha, D. Ding, W. Chong, Implementation of Surface Modified Carbon Cloth Electrodes with Biochar Particles in Microbial Fuel Cells, 2018, p. 5075, https://doi.org/10.1080/15435075.2018.1529576.
[30] C. Forrestal, P. Xu, Z. Ren, Sustainable desalination using a microbial capacitive desalination cell, Energy Environ. Sci. 5 (2012) 7161–7167, https://doi.org/10.1039/c2ee21121a.
[31] C. Xing, D. Jiang, L. Tong, K. Ma, Y. Xu, K. Xie, Y. Wang, MXene@Poly(diallyldimethylammonium chloride) decorated carbon cloth for highly electrochemically active biofilms in microbial fuel cells, Chemelectrochem 8 (2021) 2583–2589, https://doi.org/10.1002/celc.202100455.
[32] J. Chen, J. Yang, K. Zhao, Y. Wu, X. Wang, Y. Zhang, Y. Zhao, R. Wang, Y. Yang, Y. Liu, Enhancing bioelectrochemical performance of two-dimensional material attached by covalent/metal organic frameworks as cathode catalyst for microbial fuel cells, Bioresour. Technol. 360 (2022), 127537, https://doi.org/10.1016/j.biortech.2022.127537.
[33] D.T.D. Weerathunga, S.M. Jayawickrama, Y.K. Phua, K. Nobori, T. Fujigaya, Effect of polytetrafluoroethylene particles in cathode catalyst layer based on carbon nanotube for polymer electrolyte membrane fuel cells, Bull. Chem. Soc. Jpn. 92 (2019) 2038–2042, https://doi.org/10.1246/bcsj.20190208.
[34] Y. Meng, S. Lu, H. Lu, Y. Ma, Y. Wu, C. Xie, W. Zhang, M. Qian, G. Li, S. Jin, N, Se doped flower-shaped hollow carbon spheres to enhance performance in supercapacitor, Mater. Lett. 304 (2021), 130623, https://doi.org/10.1016/j.matlet.2021.130623.
[35] D. Paul, M.T. Noori, P.P. Rajesh, M.M. Ghangrekar, A. Mitra, Modification of carbon felt anode with graphene oxide-zeolite composite for enhancing the performance of microbial fuel cell, Sustain. Energy Technol. Assessments 26 (2018) 77–82, https://doi.org/10.1016/j.seta.2017.10.001.
[36] R. Qiu, B. Zhang, J. Li, Q. Lv, S. Wang, Q. Gu, Enhanced vanadium (V) reduction and bioelectricity generation in microbial fuel cells with biocathode, J. Power Sources 359 (2017) 379–383, https://doi.org/10.1016/j.jpowsour.2017.05.099.
[37] J. Chen, J. Yang, Y. Wu, Y. Zhao, X. Wang, J. Wang, D. Yang, Y. Wang, Q. Wei, R. Wang, Y. Yang, Y. Liu, Three-dimensional ZIF-67 attached lamellar Ti3AlC2 combined with ZnAl-LDH as cathode catalyst for enhancing oxygen reduction reaction of microbial fuel cells, Int. J. Hydrogen Energy 47 (2022) 16262–16271, https://doi.org/10.1016/j.ijhydene.2022.03.133.
[38] R. Rajendran, G.P. Dhakshina Moorthy, H. Krishnan, S. Anappara, A study on polythiophene modified carbon cloth as anode in microbial fuel cell for lead removal, Arabian J. Sci. Eng. 46 (2021) 6695–6701, https://doi.org/10.1007/s13369-021-05402-3.
[39] Y. Wang, C. Liu, S. Zhou, R. Hou, L. Zhou, F. Guan, R. Chen, Y. Yuan, Hierarchical N-doped C/Fe3O4 nanotube composite arrays grown on the carbon fiber cloth as a bioanode for high-performance bioelectrochemical system, Chem. Eng. J. 406 (2021), 126832, https://doi.org/10.1016/j.cej.2020.126832.
[40] E.T. Sayed, H. Alawadhi, K. Elsaid, A.G. Olabi, M.A. Almakrani, S.T. Bin Tamim, G.H.M. Alafranji, M.A. Abdelkareem, A carbon-cloth anode electroplated with iron nanostructure for microbial fuel cell operated with real wastewater, Sustain. Times 12 (2020) 1–11, https://doi.org/10.3390/su12166538.
[41] H. Xu, X. Quan, Z. Xiao, L. Chen, Effect of anodes decoration with metal and metal oxides nanoparticles on pharmaceutically active compounds removal and power generation in microbial fuel cells, Chem. Eng. J. 335 (2018) 539–547, https://doi.org/10.1016/j.cej.2017.10.159.
[42] S.H. Chang, B.Y. Huang, T.H. Wan, J.Z. Chen, B.Y. Chen, Surface modification of carbon cloth anodes for microbial fuel cells using atmospheric-pressure plasma jet processed reduced graphene oxides, RSC Adv. 7 (2017) 56433–56439, https://doi.org/10.1039/c7ra11914c.
[43] S.H. Chang, J.S. Liou, J.L. Liu, Y.F. Chiu, C.H. Xu, B.Y. Chen, J.Z. Chen, Feasibility study of surface-modified carbon cloth electrodes using atmospheric pressure plasma jets for microbial fuel cells, J. Power Sources 336 (2016) 99–106, https://doi.org/10.1016/j.jpowsour.2016.10.058.
[44] C. Hu, L. Dai, Doping of carbon materials for metal-free electrocatalysis, Adv. Mater. 31 (2019) 1–17, https://doi.org/10.1002/adma.201804672.
[45] Y. Jiang, G. Cheng, Y. Li, Z. He, J. Zhu, W. Meng, H. Zhou, L. Dai, L. Wang, Superior electrocatalytic performance of porous, graphitic, and oxygen-functionalized carbon nanofiber as bifunctional electrode for vanadium redox flow battery, Appl. Surf. Sci. 525 (2020), https://doi.org/10.1016/j.apsusc.2020.146453.
[46] Y. Ma, Z. Wei, Y. Wang, Y. Ding, L. Jiang, X. Fu, Y. Zhang, J. Sun, W. Zhu, J. Wang, Surface oxygen functionalization of carbon cloth toward enhanced electrochemical dopamine sensing, ACS Sustain. Chem. Eng. 9 (2021) 16063–16072, https://doi.org/10.1021/acssuschemeng.1c03430.
[47] S. Kwon, Y. Suharto, K.J. Kim, Facile preparation of an oxygen-functionalized carbon felt electrode to improve VO2+/VO2+ redox chemistry in vanadium redox flow batteries, J. Ind. Eng. Chem. 98 (2021) 231–236, https://doi.org/10.1016/j.jiec.2021.03.049.
[48] K. Tahir, W. Miran, J. Jang, A. Shahzad, M. Moztahida, B. Kim, D.S. Lee, A novel MXene-coated biocathode for enhanced microbial electrosynthesis performance, Chem. Eng. J. 381 (2020), 122687, https://doi.org/10.1016/j.cej.2019.122687.
[49] J.H. Song, M.J. Sailor, Dimethyl sulfoxide as a mild oxidizing agent for porous silicon and its effect on photoluminescence, Inorg. Chem. 37 (1998) 3355–3360, https://doi.org/10.1021/ic971587u.
[50] J.N. Butler, Electrochemistry in dimethyl sulfoxide, J. Electroanal. Chem. 14 (1967) 89–116, https://doi.org/10.1016/0022-0728(67)80136-0.
[51] N. Shabana, A.M. Arjun, M. Ankitha, S.A. Mohandas, P. Gangadharan, P.A. Rasheed, A flexible and sensitive electrochemical sensing platform based on dimethyl sulfoxide modified carbon cloth: towards the detection of dopamine and carvedilol, Anal. Methods (2023) 685–692, https://doi.org/10.1039/d2ay01922a.
[52] M. van Loosdrecht, P. Nielsen, C. Lopez-Vazquez, D. Brdjanovic, more, Experimental Methods in Wastewater Treatment, 2016.
[53] C. Zhang, L. Fu, N. Liu, M. Liu, Y. Wang, Z. Liu, Synthesis of nitrogen-doped graphene using embedded carbon and nitrogen sources, Adv. Mater. 23 (2011) 1020–1024, https://doi.org/10.1002/adma.201004110.
[54] B. Shi, Y. Su, Y. Duan, S. Chen, W. Zuo, A nanocomposite prepared from copper(II) and nitrogen-doped graphene quantum dots with peroxidase mimicking properties for chemiluminescent determination of uric acid, Microchim. Acta 186 (2019) 1–10, https://doi.org/10.1007/s00604-019-3491-9.
[55] T.G. Avval, C.V. Cushman, S. Bahr, P. Dietrich, M. Meyer, A. Thißen, M.R. Linford, Dimethyl sulfoxide by near-ambient pressure XPS, Surf. Sci. Spectra 26 (2019), 014020, https://doi.org/10.1116/1.5053099.

[56] J. Gomez-Bolivar, I.P. Mikheenko, R.L. Orozco, S. Sharma, D. Banerjee, M. Walker, R.A. Hand, M.L. Merroun, L.E. Macaskie, Synthesis of Pd/Ru bimetallic nanoparticles by Escherichia coli and potential as a catalyst for upgrading 5-hydroxymethyl furfural into liquid fuel precursors, Front. Microbiol. 10 (2019) 1–17, https://doi.org/10.3389/fmicb.2019.01276.
[57] K. Lu, Z. Hu, J. Ma, H. Ma, L. Dai, J. Zhang, A rechargeable iodine-carbon battery that exploits ion intercalation and iodine redox chemistry, Nat. Commun. 8 (2017) 1–10, https://doi.org/10.1038/s41467-017-00649-7.
[58] P. Gangadharan, I.M. Nambi, Feasibility study of disposed LCD monitor and carbon cloth electrodes for synchronized removal/recovery of Cr6+ by microbial fuel cells, Int. J. Environ. Sustain Dev. 8 (2017) 557–560, https://doi.org/10.18178/ijesd.2017.8.8.1015.
[59] A. Pareek, J. Shanthi Sravan, S. Venkata Mohan, Fabrication of three-dimensional graphene anode for augmenting performance in microbial fuel cells, Carbon Resour, Convers 2 (2019) 134–140, https://doi.org/10.1016/j.crcon.2019.06.003.
[60] P. Gangadharan, I.M. Nambi, The performance of Cu2+as dissolved cathodic electron-shuttle mediator for Cr6+reduction in the microbial fuel cell, Sustain. Environ. Res. 30 (2020), https://doi.org/10.1186/s42834-020-00059-3.
[61] P. Zhang, X.H. Liu, K.X. Li, Y.R. Lu, Heteroatom-doped highly porous carbon derived from petroleum coke as efficient cathode catalyst for microbial fuel cells, Int. J. Hydrogen Energy 40 (2015) 13530–13537, https://doi.org/10.1016/j.ijhydene.2015.08.025.
[62] J. Choi, P. Dorji, H.K. Shon, S. Hong, Applications of capacitive deionization: desalination, softening, selective removal, and energy efficiency, Desalination 449 (2019) 118–130, https://doi.org/10.1016/j.desal.2018.10.013.
[63] T. Jafary, A. Al-mamun, H. Alhimali, M. Said, Enhanced power generation and desalination rate in a novel quadruple microbial desalination cell with a single desalination chamber, Renew. Sustain. Energy Rev. 127 (2020), 109855, https://doi.org/10.1016/j.rser.2020.109855.
[64] Y. Kim, B.E. Logan, Series assembly of microbial desalination cells containing stacked electrodialysis cells for partial or complete seawater desalination, Environ. Sci. Technol. 45 (2011) 5840–5845, https://doi.org/10.1021/es200584q.
[65] P. Gangadharan, A. Vadekeetil, R. Sibi, A. Sheelam, Concentrating nutrients and recovering water and energy from source separated urine using osmotic microbial fuel cell, Chemosphere 285 (2021), 131548, https://doi.org/10.1016/j.chemosphere.2021.131548.
[66] P. Gangadharan, R. Rajumon, R. Sibi, A. Elizbath, Osmotic urine fuel cell to recover water , energy , and nutrients along with salinity reduction, J. Appl. Electrochem. (2022), https://doi.org/10.1007/s10800-022-01738-2.
[67] K. Zuo, J. Cai, S. Liang, S. Wu, C. Zhang, P. Liang, X. Huang, A ten liter stacked microbial desalination cell packed with mixed ion-exchange resins for secondary effluent desalination, Environ. Sci. Technol. 48 (2014) 9917–9924, https://doi.org/10.1021/es502075r.
[68] K.S. Jacobson, D.M. Drew, Z. He, Use of a liter-scale microbial desalination cell as a platform to study bioelectrochemical desalination with salt solution or artificial seawater, Environ. Sci. Technol. 45 (2011) 4652–4657, https://doi.org/10.1021/es200127p.
[69] P.A. Rasheed, R.P. Pandey, R.T. Thomas, MXenes for improved electrochemical applications, 2D Mater, Energy Storage Convers (2021) 6–40, https://doi.org/10.1088/978-0-7503-3319-1ch6.
[70] M. Mashkour, M. Rahimnejad, F. Raouf, N. Navidjouy, A review on the application of nanomaterials in improving microbial fuel cells, Biofuel Res. J. 8 (2021) 1400–1416, https://doi.org/10.18331/BRJ2021.8.2.5.